Int. J. Heat Mass Transfer. Vol. 14, pp. 1631–1641. Pergamon Press 1971. Printed in Great Britain

AN EXPERIMENTAL STUDY OF ENERGY TRANSFER PROCESSES RELEVANT TO THERMAL EXPLOSIONS

S. J. BOARD, A. J. CLARE, R. B. DUFFEY, R. S. HALL and D. H. POOLE

Central Electricity Generating Board, Berkeley Nuclear Laboratories, Berkeley, Glos., England

(*Received* 27 *August* 1970 *and in revised form* 2 *November* 1970)

Abstract—Energy transfer and vapour production processes have been studied in an experiment involving the transient heating of a metal foil under water. Data were obtained on temperature, pressure and heat flux with a time resolution of $\leqslant 10$ μs over the range of foil temperatures 100–900°C and of water subcoolings 20–80°C. Both unstable and stable energy transfer processes have been shown to occur at temperatures above the nucleate boiling region and relevant quantitative heat flux data have been obtained.

NOMENCLATURE

$A, B, C,$	constants of integration;
$f,$	oscillation frequency;
$G,$	gas constant;
$k_l,$	liquid thermal conductivity;
$K_1, K_2, K_3,$	constants defined in text;
$l,$	effective piston length;
$L,$	latent heat;
$m,$	mass of vapour;
$P_v,$	pressure of vapour;
$P_\infty,$	pressure at infinity;
$Q_T,$	heat flux from target;
$Q_C,$	condensation heat loss;
$R,$	radius of target;
$s_1, s_2,$	defined in text;
$T_{sat},$	saturation temperature;
$T_\infty,$	bulk liquid temperature;
$t,$	time;
$x,$	displacement of vapour blanket from equilibrium position;
$\alpha,$	thermal diffusivity of liquid;
$\delta,$	equilibrium vapour blanket thickness;
$\rho_l,$	liquid density;
$\rho_v,$	vapour density;
$\rho_\infty,$	vapour density at pressure P_∞;
$\tau,$	duration of heating pulse.

1. INTRODUCTION

THE POSSIBILITY of a thermal explosion resulting from the mixing of molten fuel and coolant in an accident situation is an important problem in the study of the safety of liquid cooled reactors, and as such has received considerable attention. The particular context of the current work has been the safety of liquid metal cooled fast reactors, in which, because of the high power density and low operating pressures, coolant voiding and re-entry followed by fuel-coolant thermal interactions become a critical part of the safety problem.

Early work on thermal explosions [1,2] has shown that during the explosion the molten material becomes finely dispersed, greatly increasing the available surface area. The dispersal mechanisms have been studied directly in subsequent experiments [3–5].

This is only part of the problem, however. Even with the enhanced surface area, the energy transfer rates which can be deduced to be necessary to permit explosive generation of high pressures are very much greater than those observed in steady boiling processes. It is therefore also necessary to obtain measurements of heat transfer and vapour production rates

under appropriate transient conditions. These measurements may be made with solid materials, since it is unlikely that the processes will differ fundamentally from those occurring with molten debris. The use of solid materials permits temperatures and heat fluxes to be monitored directly.

The temperature range 100–200°C has been adequately converted by a number of transient boiling experiments (e.g. [6–8]), but the postulated mechanism of heat transfer (evaporation of a microlayer of water from the base of growing bubbles) is not applicable to materials above the critical temperature of the coolant. However, there is substantial evidence that thermal explosions can occur under these circumstances.

At temperatures significantly above the nucleate boiling region, experimental studies of forced convection cooling [9, 10] and relatively slow transient heating [11] have produced evidence of the existence of several different types of energy transfer process, and some quantitative heat flux data has also been obtained but with limited time resolution.

The present experiment was designed to investigate the nature of the energy transfer and vapour production processes occurring over short timescales from high temperature metal foils under water by measurement of temperatures, pressures and vapour generation rates. The ultimate aim of the experiment is the determination of the thermal efficiency of vapour production under the conditions relevant to a thermal explosion.

2. EXPERIMENTAL TECHNIQUES

The main features of the experiment, in which a metal foil was heated under water by a pulsed ruby laser, have been described previously [5]. An image of the front face of a Czochralski S.I.Q. coreless ruby was focused on to the foil target, achieving a maximum uniform (±20 per cent) absorbed power density of the order of 60 kW cm^{-2} over a 6 mm dia. heated area. The power was varied by means of neutral density filters in order to preserve the uniformity of beam distribution. The target was made of nickel foil of thickness 0·001 cm. The front to back surface temperature equalisation was very fast (~ 3 μs for equalisation within ±15 per cent) compared with the rate of temperature changes in the experiment and hence the bulk foil temperature was sensibly uniform at all times.

For the experiments reported here in which the target foil remains unmelted, the temperature was measured by a resistance thermometry technique in which a constant current was passed through the foil and the temperature was determined from the potential between two leads within the target area (see Fig. 1). The

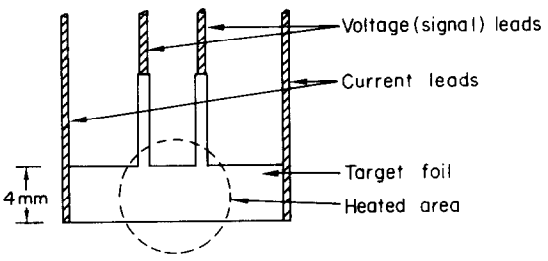

FIG. 1. Target assembly.

response time of this system was limited by the time for temperature equalisation.

The absorbed laser power was deduced from the target heating rate in air, when the losses were negligible; the heat fluxes in the experiment were deduced from the observed cooling rates of the foil (after the end of the heating pulse) knowing its thermal capacity. The laser was used in its normal mode, in which the overall pulse length is 1 ms. The length of the heating pulse used was controlled by a rotating disc beam chopper. In conjunction with neutral density filters, this permitted independent control of the target heating rate and peak temperature. The conditions investigated have involved heating rates of 1–10°C μs^{-1} and peak temperatures of 100–900°C.

The pressure produced in the open vessel of water by vapour generation was monitored with a Kistler type 603B pressure transducer (maxi-

mum frequency response 250 kHz) which was mounted within 2 cm of the target to provide an adequate ratio of pressure signal level to vessel resonance effects. Photographic data has been obtained using a Fastax camera (7600 frames s^{-1}) and a Barr and Stroud C.P.5 framing camera. The latter has a rotating mirror which was synchronised with the beam chopper by timing pulses gated in a simple nucleonic coincidence system: the output of the latter was used to trigger the laser. The mirror speed was chosen to give an observation time of about 300 μs and framing period of 3 μs. High resolution single photographs were also taken, using a 35 mm camera with an open shutter technique with a fast (~ 10 μs) xenon discharge lamp.

The analogue data (beam power, foil temperature, pressure transducer signal) were displayed on an oscilloscope and also recorded by a high speed digitising system based on a small digital computer [12]. A block diagram of the experimental arrangement is shown in Fig. 2.

3. RESULTS AND DISCUSSION

3.1 *Identification of energy transfer processes*

Results obtained from events covering the range of target temperatures 100–900°C and of water temperatures 20–80°C indicate the existence of several distinct processes of transient energy transfer, illustrated schematically in Fig. 3 and summarised in Table 1. These are:

(a) *Nucleate boiling region.* This occurs near the beginning of the heating pulse for all events and for fast (200 μs) transients in cold water continues until target temperatures of about 200°C are reached. Maximum heat fluxes of about 3·6 kW cm^{-2} are observed under these conditions.

(b) *Oscillating vapour blanket region.* For target temperatures above the nucleate boiling temperature range but below about 450°C in hot water and 350°C in cold water, the dominant heat loss mechanism involves the periodic collapse of a vapour blanket on the target. (The critical temperature of water is 374°C.) This produces repeated large heat fluxes for short periods (3–10 kW cm^{-2} for 10–30 μs). A typical event record and a sequence of photographs of a collapsing blanket are shown in Fig. 4. The blanket collapse is evident from the peaks in the pressure trace as well as the steps in the temperature trace on the event record.

(c) *High temperature region.* For target tem-

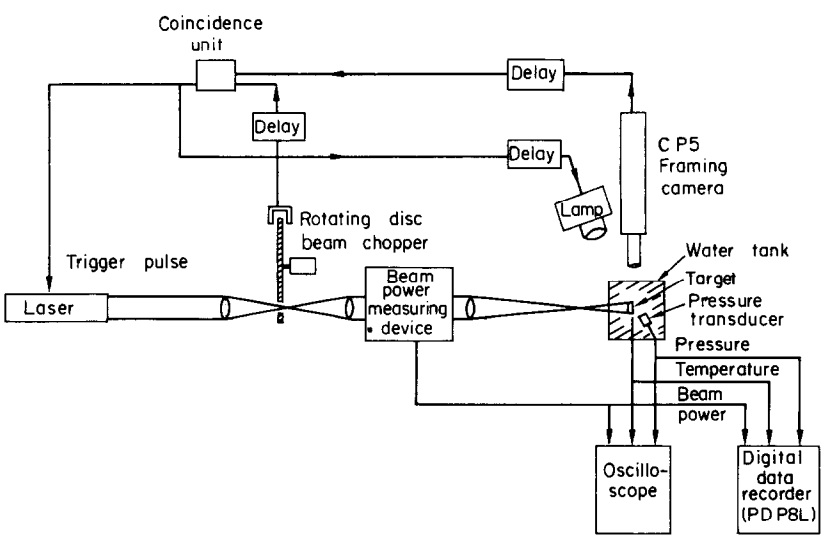

FIG. 2. Schematic diagram of experimental arrangement with CP5 framing camera.

Table 1. Some results characterising the various energy transfer regions

Region	Target temperature (°C)	Subcooling (°C)	Heat flux (kW cm^{-2})	Timescale
Nucleate boiling	200	74	3·6	averaged over 100 μs after heating pulse
	180	48	2·3	averaged over 100 μs after heating pulse
Oscillating blanket	270	27	9	~10 μs
	$270 < T < 400$	27	<1	~30 μs
High temperature region	$T > 500$	<30	≤0·3 (flux proportional to subcooling)	few ms
	$T > 500$	>30	~1	~100 μs

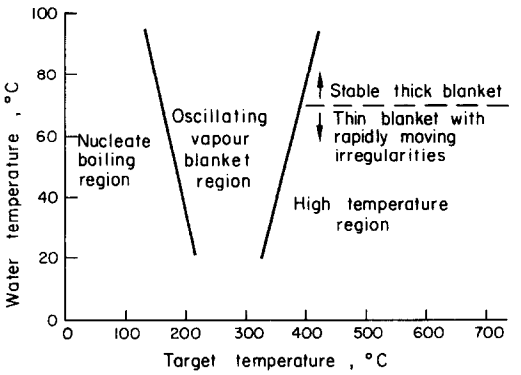

FIG. 3. Schematic diagram of heat transfer regions.

peratures of above about 500°C in hot water the vapour blanket rapidly stabilises, permitting only low steady heat fluxes (<300 W cm^{-2}). The photograph in Fig. 5 shows that the blanket is fairly thick but irregular; the pressure and temperature traces show that the periodic collapse has disappeared, leaving only a slow, small amplitude oscillation.

For targets at similarly high temperatures in cold water, however, (Fig. 6) the vapour blanket appears to be much thinner, permitting correspondingly greater heat fluxes (~ 1 kW cm^{-2}), and the irregularities are of a very much smaller scale (~ $\frac{1}{10}$ mm). The edge-on photograph of the foil in Fig. 6 shows clearly that the irregularities extend significantly into the liquid region, some being detached completely from the main body of the blanket.

The oscillating vapour blanket and high temperature regions are discussed in detail in sections 3.2 and 3.3 respectively. A brief discussion of the nucleate boiling region is included in section 3.4.

3.2 *Oscillating vapour blanket region*

3.2.1 *Oscillation frequency.* The periodic collapse of a vapour blanket has been observed to occur in steady-state transition boiling [13], in forced convection cooling [10] as well as in transient boiling experiments [6, 11]. Hall and Harrison [6] suggested that the period of oscillation was determined by the pressure wave transit time in the vessel. Detailed investigation of the factors determining the vapour blanket oscillation in the present experiment has shown that the oscillation period was independent of the size of the experimental vessel for cubic vessels with sides of length between 5 and 100 cm, but was very strongly dependent on the temperature of the water. A graph of oscillation frequency over the second cycle against water subcooling is shown in Fig. 7. It may be seen that the frequency increases linearly with increasing subcooling for water temperatures of between 90°C and 25°C.

This result may be interpreted qualitatively in terms of the generation at each blanket collapse of a fixed mass of vapour which must be completely condensed before the next collapse, so

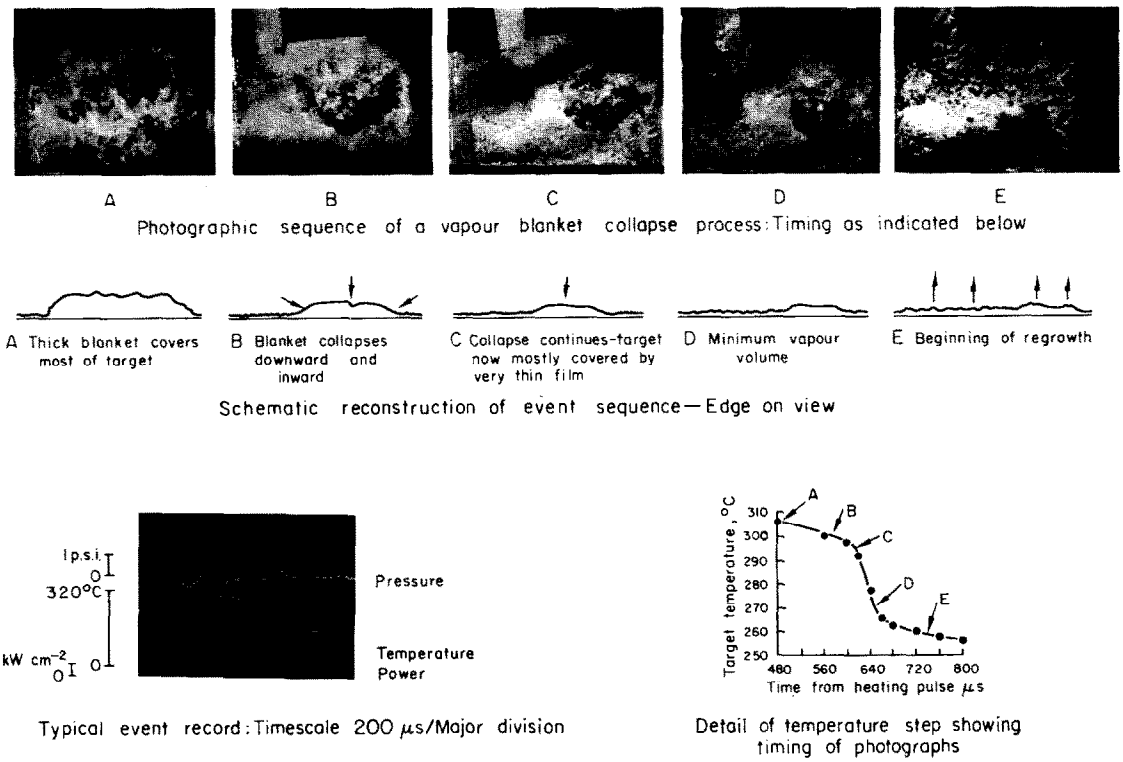

FIG. 4. Oscillating vapour blanket region (20°C subcooling).

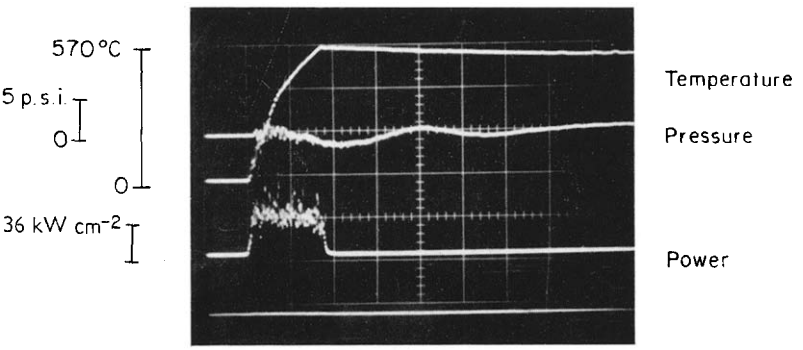

Typical event record
Timescale: 200 μs/Major division

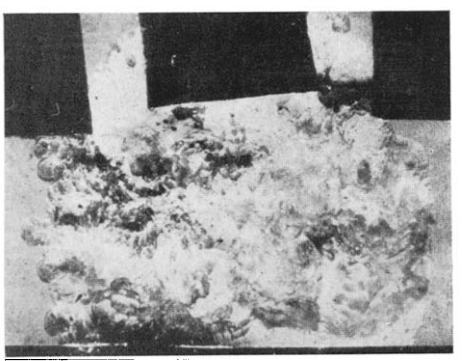

Appearance of vapour blanket at end of heating pulse

FIG. 5. High temperature region at low subcoolings (20°C).

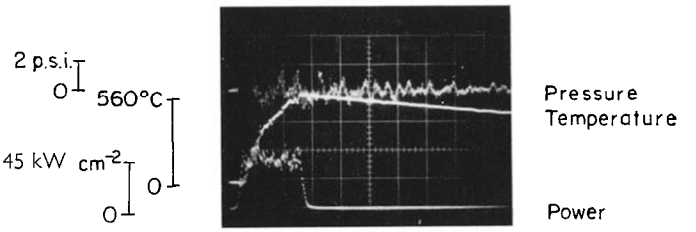

Record of event at 74°C subcooling
Timescale: 100 μs/Major division

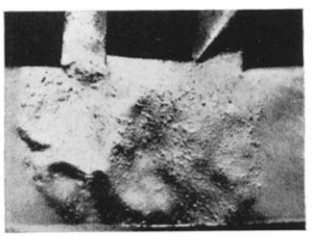

Appearance of vapour blanket at end of heating pulse

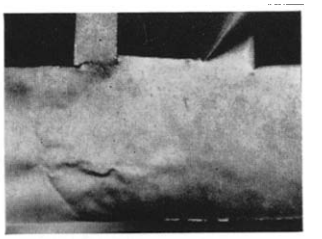

Unheated target

FIG. 6. High temperature region at high subcoolings.

(a) Initial nucleate boiling

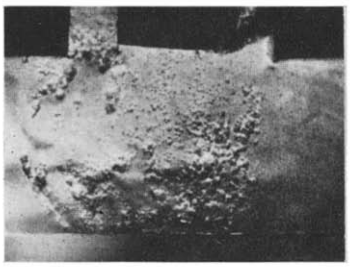

(b) Bubble coalescence

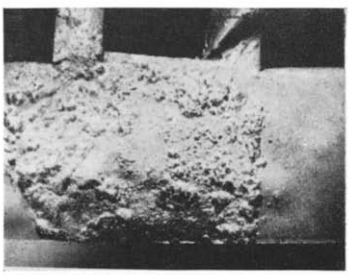

(c) Condensation period

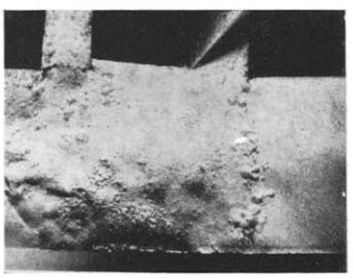

(d) Stable thin film region

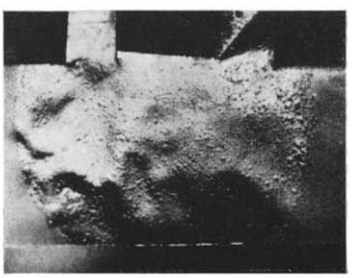

FIG. 12. Event sequence in which target reaches 500°C at 80°C subcooling.

that the product of condensation loss and inter-collapse period is constant (i.e. frequency is proportional to subcooling).

For the case of small amplitude blanket oscillations, the linear variation may also be deduced from the highly simplified model described in the appendix which considers the oscillation as a small perturbation in the thickness of an equilibrium vapour blanket. The predictions of the model are fitted to the data in Fig. 7 by the choice of the equilibrium film thickness of 3×10^{-3} cm at 70°C.

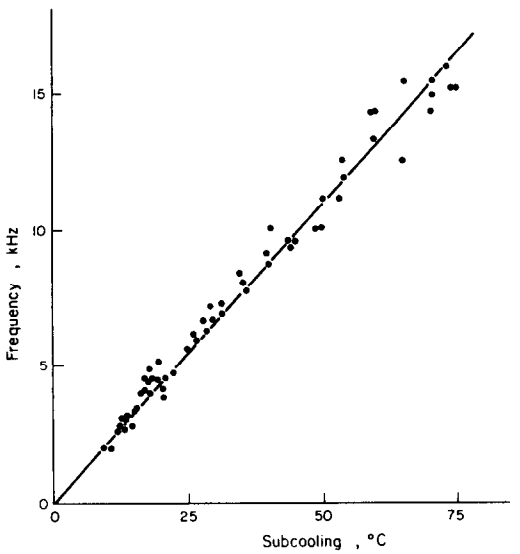

FIG. 7. Oscillation frequency/subcooling for target temperature 400°C.

The effect of inertial coupling of the water to the vapour blanket in the model results in a predicted cube root variation of period with radius of heated target area; a logarithmic plot of period against target radius is shown in Fig. 8 where the straight line has a slope of $\frac{1}{3}$.

3.2.2 *Oscillation amplitude and temperature step size.* If the amplitude of the vapour blanket oscillation is comparable to the blanket equilibrium thickness, periodic contact between the liquid and foil may be permitted, resulting in

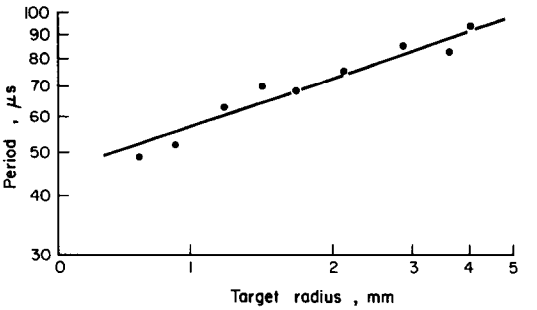

FIG. 8. Oscillation period/target radius for 25°C water, 200°C target.

large heat fluxes and distinct foil temperature steps. The conditions under which the step size is measurable may be seen from Fig. 9, which

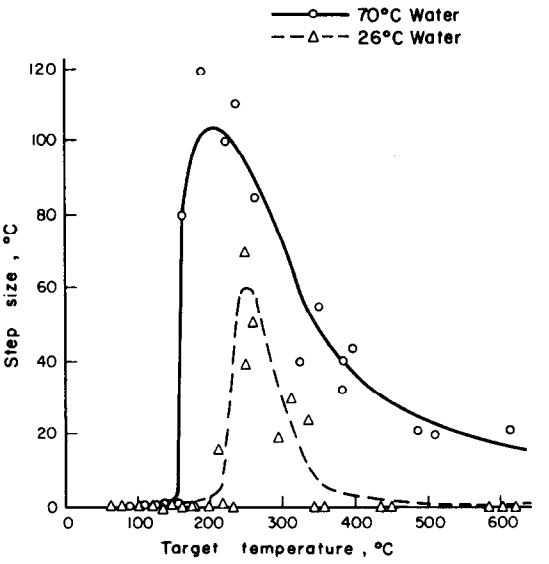

FIG. 9. Temperature step size/target temperature.

shows the size of the first collapse temperature step as a function of both target and water temperatures. In cold water there is only a very narrow range of target temperatures (220–320°C) for which a measurable step structure occurs, whereas in hotter water the range is increased (120–500°C) and the step size is increased also.

The presence of a maximum step size at a

target temperature of about 200°C suggests that the energy transfer during collapse below this temperature may be by means of a nucleate boiling process (see section 3.4). The photographs in Fig. 4 show that during collapse at target temperatures of about 350°C, the target is covered by a thin vapour film not unlike the stable film on high temperature targets at high subcoolings (Fig. 6).

The water temperature variation of step size is the reverse of that observed for both nucleate and film boiling heat fluxes, and it is therefore reasonable to expect that the step size variation reflects the variation of initial conditions for the collapse, which will depend on the blanket oscillation amplitude (for instance, impact velocity may be greater for higher amplitude oscillations).

Information on the water temperature variation of oscillation amplitude is not easily obtained photographically (see section 4). However, independent information on the amplitude may be obtained from measurements of the size of the pressure peak associated with the initial vapour blanket growth rate. The size of the measured pressure peak is found to increase with water temperature over the range 20–80°C, probably reflecting the diminishing condensation loss at high temperatures.

Thus the amplitude of oscillation may be expected to increase with water temperature, a result which is consistent with the observed increase in target temperature step size.

3.2.3 *Step heat fluxes.* The heat fluxes occurring during a blanket collapse process have been calculated from the slope of the temperature traces for events at low sub-coolings where there is photographic evidence that the collapse occurs fairly uniformly over the target. However, the values of heat flux should be interpreted as lower limits, since it has been assumed that the whole heated surface area (both sides) is involved for the full duration of the step.

A graph of step heat flux against target temperature for water at 73°C is shown in Fig. 10. The curve rises to a maximum of about

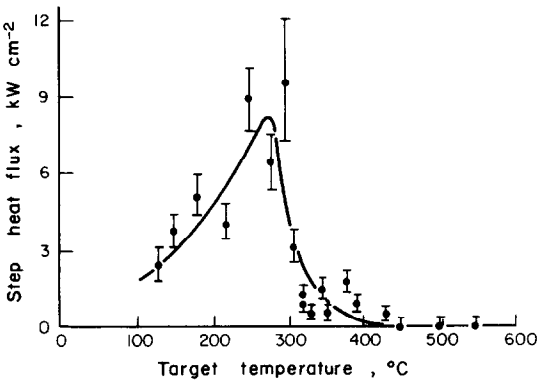

FIG. 10. Step heat flux/target temperature.

9 kW cm^{-2}, falls sharply at a target temperature of 270°C to about 1 kW cm^{-2}, then drops slowly till the steps disappear above about 500°C.

The rapid fall in heat flux above a temperature of 270°C may be interpreted as due to the onset of the Leidenfrost effect. The apparent Leidenfrost temperature of 270°C does not differ greatly from the value of 237°C deduced by Cumo and Pitimada [14] from the cooling rate of a nickel plate under the impact of a water jet, or that shown by the results of Pedersen (260°C) obtained by a droplet impact technique [15]. It should be noted that there is likely to be an impact velocity dependence of Leidenfrost temperature which would affect all these measurements.

3.3 *High temperature region*

3.3.1 *Low subcoolings.* For target temperatures significantly above the Leidenfrost temperature at low subcoolings, the initial vapour blanket oscillations decay rapidly and the target cools slowly and steadily indicating that a stable film-blanketed regime is established. Under these conditions (target > 500°C, subcooling < 30°C) the heat flux from the target at the end of the heating pulse is very low and shows a simple linear relation to subcooling (Fig. 11). The straight line shows the calculated conduction loss through a thermal diffusion boundary

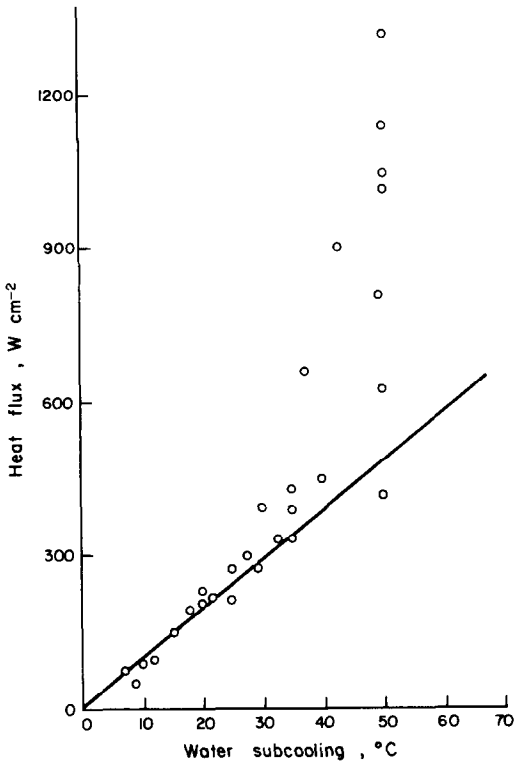

FIG. 11. Heat flux/subcooling

layer (thickness λ) in the water when the liquid/vapour interface is maintained at the saturation temperature. The heat loss is given by

$$Q_c = k_l \frac{(T_{sat} - T_\infty)}{\lambda}$$

where $\lambda = (\alpha\tau)^{\frac{1}{2}}$.

The agreement of the theoretical prediction with the experimental results tends to confirm the hypothesis of a stable thermal diffusion boundary layer in the liquid.

3.3.2 *High subcoolings.* For subcoolings greater than about 30°C however, the heat fluxes become more variable, and are considerably greater than those predicted by the above relationship. This indicates that there must be either a temporal or spatial disturbance of the thermal boundary layer. There is evidence from the high frequency component of the pressure traces (Fig. 6), and from some of the C.P.5 framing camera photographs that the irregularities on the surface of the vapour blanket in this region undergo fast, bubble-like growth and collapse processes. These may be expected to produce disturbance of the boundary layer if the scale of the irregularities is comparable with the boundary layer thickness, but it is unlikely that variations in the saturation temperature due to blanket pressure changes (i.e. temporal boundary layer disturbance) would significantly alter the heat transfer rates.

3.4 *Average heat flux as a function of target temperature at high subcoolings*

The condition of high subcooling is probably the most directly relevant to a full scale thermal interaction when the explosive pressures ensure that the local subcooling will be large even if the interacting coolant is near its normal boiling point.

The sequence of pictures of a typical event at 80°C subcooling in Fig. 12 illustrates an event in which the target is heated to 500°C. The initial nucleate boiling region is followed by a period of bubble coalescence in which condensation appears to reduce the total volume of vapour, leaving only a thin film covering the target for the remainder of the heating pulse and most of the cooling period. A graph of average heat flux measured during the 100 μs after the end of the heating pulse as a function of target temperature for subcoolings of 48° and 74°C is shown in Fig. 13. As the maximum target temperature rises above 100°C the nucleate boiling heat flux increases, reaching a maximum (3·6 kW cm^{-2} for 74°C subcooling) at a target temperature of about 200°C. This corresponds to the critical heat flux observed by Tachibana *et al.* [7] and is directly comparable to the maximum flux recorded by Hall and Harrison [6] during the exponential heating of a platinum strip at 80°C subcooling (2·9 kW cm^{-2} at 185°C for τ = 700 μs).

For target temperatures of above 200°C, the average flux decreases with increasing target

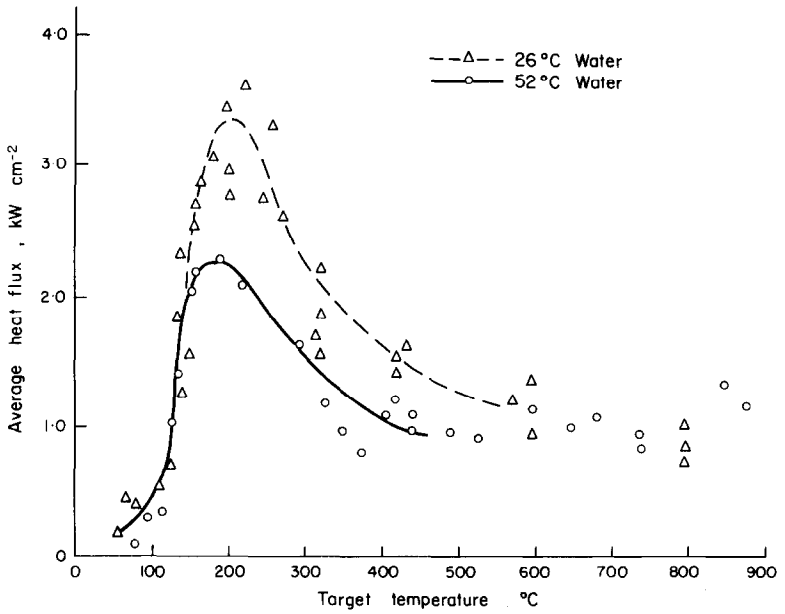

FIG. 13. Average heat flux/target temperature.

temperature, a phenomenon also observed at somewhat lower temperatures in pool boiling experiments and commonly called transition boiling. From the temperature step size analysis in cold water (Fig. 9, lower curve) it may be seen that the region of observable step size (220–320°C) corresponds in target temperature to the region of decreasing average flux. This lends support to the interpretation of steady-state transition boiling in terms of alternating periods of unstable nucleate and film boiling [16, 17].

For target temperatures of above 500°C (also discussed in Section 3.2) the average heat flux appears to be not strongly dependent on either target temperature or subcooling (for subcoolings above 48°C) though the data show considerable scatter. The mean value of the flux under these conditions is approximately 1 kW cm^{-2}.

3.5 *Vapour film thicknesses*

Measurements of heat fluxes from a foil target have been obtained under a wide variety of conditions, but further information on the vapour volumes associated with the fluxes is needed to determine the physical nature of the heat transfer processes involved. Direct measurement of the volume of vapour on the target surface from edge-on photographs of a foil is impracticable because of the effects of thermal buckling and the very irregular surface of the vapour. Measurements have been made of the average vapour film thickness around wires but it should be noted that the heat transfer processes on a wire may be significantly different from those on a foil. The wire measurements indicate that the vapour film thicknesses are in the range 3–20 $\times 10^{-3}$ cm, values which are in general 1 or 2 orders of magnitude greater than those which could support the observed fluxes from wires ($\sim$1 kW cm^{-2}) by conduction alone. A similar conclusion may be tentatively drawn for foils from the rough estimates of blanket thickness which are possible from the face-on photographs.

Postulating a 'heat pipe' mechanism to provide the necessary increase in energy transfer rate across the vapour requires the existence of water within the observed vapour volume;

evidence for this in the blanket surrounding foil targets can be seen from Fig. 6 where there is an apparent water/vapour mixing process occurring at the blanket surface. There is no evidence of such mixing from the wire photographs but this may be due to the more limited resolution. Another possible mechanism for injecting water into the vapour region is the initial coalescence of bubbles formed during the nucleate boiling period [18].

4. CONCLUSIONS

An experiment involving the fast transient heating of a metal foil under water in which measurements of temperature, pressure and heat flux were made with instrumental response times $\leqslant 10$ μs has enabled some new qualitative and quantitative data to be obtained relevant to several distinct types of energy transfer process.

The nucleate boiling region has been observed to extend up to 200°C with heat fluxes as high as 3·6 kW cm^{-2} for 200 μs transients at 80°C subcooling. Above the nucleate boiling region, but below about 500°C at low subcoolings, an oscillating vapour blanket is formed; this permits collapse heat fluxes up to 9 kW cm^{-2} for a few tens of microseconds at temperatures below 270°C (identified as the Leidenfrost temperature). The pressures produced by the collapsing vapour blanket process may be important in the dispersal of molten material in a thermal explosion. Significantly above this temperature, a stable but irregular vapour blanket is formed permitting heat fluxes which, at low subcoolings, are predicted by the theoretical conduction loss across a thermal diffusion boundary layer in the water. At higher subcoolings, the blanket is thinner and the heat fluxes (~ 1 kW cm^{-2}) are above the theoretical level of conduction loss in the water. It is postulated that the necessary disturbance of the boundary layer is associated with small rapidly moving irregularities in the blanket. There is some evidence that the blankets are in general too thick to support the observed fluxes at high target temperatures by conduction across a pure vapour layer; a two-phase blanket which supports the flux by a heat pipe mechanism is proposed.

REFERENCES

1. G. Long, Explosions of molten aluminium in water—cause and prevention, *Metal Progress* **71**, 107–112 (1957).
2. R. W. Wright, Kinetic studies of heterogeneous water reactors, Physical Electronics Lab, TRW Systems, Report STL 372-30, 62–74 (1965).
3. K. Flory, R. Paoli and R. Mesler, Molten metal–water explosions, *Chem. Engng Prog.* **65**, 50–54 (1969).
4. D. H. Cho, D. R. Armstrong and W. H. Gunther, Molten material–coolant interactions, *Trans. Am. Nucl. Soc.* **13**, 385 (1970).
5. A. J. Clare, R. B. Duffey, R. S. Hall, T. S. Playle and D. H. Poole, Metal–coolant thermal interactions at high temperatures: preliminary results from a laser heating experiment, CEGB Report RD/B/N1448 (1969).
6. W. B. Hall and W. C. Harrison, Transient boiling of water at atmospheric pressure, Proc. 3rd Int. Heat Transfer Conf., Inst. Mech. Eng., Chicago, pp. 193–203 (1966).
7. F. Tachibana, M. Akiyama and H. Kawamura, Heat transfer and critical heat flux in transient boiling, an experimental study in saturated pool boiling, *J. Nucl. Sci. Tech.* **5**, 117–126 (1968).
8. A. O. Yesin and D. E. Jeffers, Bubble growth in transient pool boiling, *J. Br. Nucl. Engng Soc.* **8**, 267–274 (1969).
9. F. J. Walford, Transient heat transfer from a hot nickel sphere moving through water, *Int. J. Heat Mass Transfer* **12**, 1621–1625 (1969).
10. L. C. Witte, J. W. Stevens and P. J. Henningson, The effect of subcooling on the onset of transition boiling, *Trans. Am. Nucl. Soc.* **12**, 806 (1969).
11. R. C. Pottinger. Private communication (1970).
12. A. J. Clare and W. N. Walker, A high speed multi-channel data acquisition system using a small digital computer, CEGB Report RD/B/N1683 (1970).
13. J. W. Westwater and J. W. Santangelo, A photographic study of boiling, *Ind. Engng Chem.* **47**, 1605–1610 (1955).
14. M. Cumo and D. Pitimada, Determination of the Leidenfrost temperature, 22nd National A.T.I. Congress, Rome, translated by A. Crozy, CONF. 670990-1 [NSA27(21)4345] (1967).
15. C. O. Pedersen, An experimental study of the dynamic behaviour and heat transfer characteristics of water droplets impinging on a heated surface, *Int. J. Heat Mass Transfer* **13**, 279–381 (1970).
16. P. J. Berenson, Experiments on pool boiling heat transfer, *Int. J. Heat Mass Transfer* **5**, 985–999 (1962).
17. S. G. Bankoff and V. S. Mehra, Quenching theory for transition boiling, *Ind. Engng. Chem. Fundamentals* **1**, 38–40 (1962).
18. N. J. M. Rees, Private communication (1970).

APPENDIX

Simplified Theory for Vapour Blanket Oscillation

Assumptions and approximations

1. The fluid is non-viscous and incompressible.
2. The vapour density is negligible compared to the liquid density.
3. The specific heats are negligible compared to the latent heat.
4. Any departures from equilibrium values of δ, P_v, ρ_v are small enough to neglect terms higher than first order.
5. The heat flux from the target is inversely proportional to the blanket thickness i.e. $Q_T = K_1/\delta$.
6. The condensation loss to bulk water is proportional to subcooling i.e. $Q_c = K_2(T_{sat} - T_\infty)$.
7. $1/T\,(\partial T/\partial P)_{sat}$ is negligible compared with $1/\rho\,(\partial\rho/\partial P)_{sat}$ so that the expression $P_v = \rho_v G T_\infty$ holds for small changes along the saturation curve.

Theory

Consider the target to be covered by a vapour blanket of thickness δ which maintains equilibrium between the heat from the target and the heat lost to the bulk water, i.e.

$$\frac{K_1}{\delta} = K_2(T_{sat} - T_\infty). \tag{1}$$

If the blanket is perturbed by a small displacement x, then the nett vapour generation rate is

$$\dot{m} = \frac{\Delta Q_T}{L} = -\frac{K_1 x}{\delta^2 L}. \tag{2}$$

But

$$m = \rho_v(\delta + x)$$

so that to first order

$$\dot{m} = \delta\dot{\rho}_v + \dot{x}\rho_\infty. \tag{3}$$

From (2) and (3) we have

$$-\frac{K_1 x}{\delta^2 L} = \delta\dot{\rho}_v + \dot{x}\rho_\infty. \tag{4}$$

For small changes along the saturation curve (see assumption 7)

$$\dot{P}_v = \dot{\rho}_v G T_\infty. \tag{5}$$

We assume that inertial coupling in the system may be represented by an effective piston of water of length l which moves with the vapour interface; if geometric similarity holds we may write

$$l = K_3 R.$$

The equation of motion is thus

$$P_v - P_\infty = \rho_l K_3 R\ddot{x}$$

or

$$\dot{P}_v = \rho_l K_3 R\dddot{x}. \tag{6}$$

From (4)–(6)

$$\frac{\delta\rho_l K_3 R}{G T_\infty}\dddot{x} + \rho_\infty\ddot{x} + \frac{K_1}{\delta^2 L}\dot{x} = 0.$$

The solution to this third order differential equation in x is

$$x = A\exp[(s_1 + s_2)t] + \exp\left[\left(\frac{s_1 + s_2}{2}\right)t\right] \times B\sin\left[\frac{\sqrt{3}}{2}(s_1 - s_2)t\right] + C\cos\left[\frac{\sqrt{3}}{2}(s_1 - s_2)t\right] \tag{7}$$

where

$$s_1 = \left\{\frac{-K_1 G T_\infty}{\delta^3\rho_l L K_3 R}\left[-\frac{1}{2} + \left(\frac{\rho_\infty^2 G T\delta^3 L^2}{27\rho_l K_3 R} + \frac{1}{4}\right)^{\frac{1}{2}}\right]\right\}^{\frac{1}{3}}$$

and

$$s_2 = \left\{\frac{-K_1 G T_\infty}{\delta^3\rho_l L K_3 R}\left[-\frac{1}{2} - \left(\frac{\rho_\infty^2 G T\delta^3 L^2}{27\rho_l K_3 R} + \frac{1}{4}\right)^{\frac{1}{2}}\right]\right\}^{\frac{1}{3}}.$$

For the case where $\dot{x}\rho_\infty$ is negligible compared with $\delta\dot{\rho}_v$

$$s_1 = \left(\frac{-K_1 G T_\infty}{\delta^3\rho_l L K_3 R}\right)^{\frac{1}{3}}$$

$$s_2 = 0.$$

Equation (7) describes the disturbed vapour blanket undergoing a damped harmonic oscillation as it returns exponentially to its equilibrium position. The oscillation frequency is

$$f = \frac{\sqrt{3}}{4\pi\delta}\left(\frac{G T_\infty K_1}{\rho_l L K_3 R}\right)^{\frac{1}{3}}. \tag{8}$$

Substituting for δ from equation (1)

$$f = \left[\frac{\sqrt{3}}{4\pi}K_2\left(\frac{G T_\infty}{\rho_l L K_3 K_1^2 R}\right)^{\frac{1}{3}}\right](T_{sat} - T_\infty) \tag{9}$$

Substituting in equation (8) for the case $T_\infty = 70°C$ the values:

$T_{sat} = 100°C$
$G = 0{\cdot}46\ J°K^{-1}\,g^{-1}$
$\rho_l = 1\ g\,cm^{-3}$
$L = 2300\ J\,g^{-1}$
$K_3 = 1$
$R = 0{\cdot}3$ cm
$\dfrac{K_1}{\delta_{T=70}} = K_2(T_{sat} - T_\infty) = 300W\,cm^{-2}$ (from Fig. 11)
$f = 6{\cdot}5$ kHz (from Fig. 7),

enables the values of $\delta_{T=70}$ and K_1 to be determined.

Equation (9) then predicts the linear relation between frequency and subcooling represented by the straight line drawn in Fig. 7. Agreement is maintained with the experimental data over a wide range.

ÉTUDE EXPÉRIMENTALE DES PROCESSUS DE TRANSFERT D'ÉNERGIE AU COURS D'EXPLOSIONS THERMIQUES

Résumé—Les processus de transfert d'énergie et de production de vapeur ont été étudiés dans une expérience concernant le chauffage transitoire d'une feuille métallique dans l'eau. Des résultats sont obtenus sur la température la pression et le flux thermique avec une résolution en temps $\leqslant 10\,\mu s$ pour une gamme de température de la surface 100 – 900°C et de sous refroidissement de l'eau 20 – 80°C. On a obtenu aussi bien des processus instables que stables de transfert d'énergie à des températures au-dessus de la région d'ébullition nucléée et des flux thermiques correspondant ont été mesurés.

EINE EXPERIMENTELLE UNTERSUCHUNG VON ENERGIETRANSPORTPROZESSEN, WIE SIE BEI THERMISCHEN EXPLOSIONEN AUFTRETEN

Zusammenfassung—Es wurden Energietransport- und Dampferzeugungsprozesse durch instationäre Aufheizung einer Metallfolie unter Wasser experimentell untersucht. Bei einer Zeitauflösung von $\leqslant 10\,\mu s$ konnten Messwerte von Temperatur, Druck und Wärmestrom in Bereichen der Folientemperatur von 100–900°C und der Wasserunterkühlung von 20–80°C erhalten werden. Es zeigte sich, dass sowohl instabile als auch stabile Energietransportprozesse bei Temperaturen oberhalb des Blasensiedebereichs auftreten. Dies wird durch dementsprechende quantitative Werte für den Wärmestrom belegt.

ЭКСПЕРИМЕНТАЛЬНОЕ ИССЛЕДОВАНИЕ ПРОЦЕССА ЭНЕРГОПЕРЕНОСА ПРИ ТЕПЛОВЫХ ВЗРЫВАХ

Аннотация—Процессы энергопереноса и производства пара изучалиср экспериментально при нестационарном нагреве металлической фольги под водой. Получены данные для температуры, давления и теплового потока с разрешением во времени $\leqslant 10\,\mu c$ в диапазоне температур фольги 100–900°C и воды 20–80°C. Показано, что при температурах выше температур пузырькового кипения могут иметь место как нестационарные, так и стационарные процессы энергопереноса. Получены соответствующие количественные оценки для теплового потока.